

TITLE CALIBRATION OF SCINTILLATION DETECTORS FOR MeV CHARGED FUSION PRODUCTS

**AUTHOR(S) M. Tuszewski P-1
S. Zweben Princeton Plasma Physics Laboratory**

**SUBMITTED TO Ninth Topical Conference on High-Temperature Plasma Diagnostics
Santa Fe, New Mexico**

15-19 March 1992

DISCLAIMER

This report was prepared as an account of work sponsored by an agency of the United States Government. Neither the United States Government nor any agency thereof, nor any of their employees, makes any warranty, express or implied, or assumes any legal liability or responsibility for the accuracy, completeness, or usefulness of any information, apparatus, product, or process disclosed, or represents that its use would not infringe privately owned rights. Reference herein to any specific commercial product, process, or service by trade name, trademark, manufacturer, or otherwise does not necessarily constitute or imply its endorsement, recommendation, or favoring by the United States Government or any agency thereof. The views and opinions of authors expressed herein do not necessarily state or reflect those of the United States Government or any agency thereof.

By acceptance of this article, the publisher recognizes that the U.S. Government retains a nonexclusive, royalty-free license to publish or reproduce the published form of this contribution, or to allow others to do so, for U.S. Government purposes.

The Los Alamos National Laboratory requests that the publisher identify this article as work performed under the auspices of the U.S. Department of Energy.

MASTER



Calibration of Scintillation Detectors for MeV Charged Fusion Products

M. Tuszewski

Los Alamos National Laboratory, Los Alamos, NM 87545

S. J. Zweben

Princeton Plasma Physics Laboratory, Princeton, NJ 08544

Abstract

The light output of ZnS scintillators used to detect escaping fusion products in the TFTR Tokamak is studied with 0.5 MeV alpha and 3 MeV proton beams. The emitted light first increases linearly with beam current and then saturates. In all cases investigated, the onset of the saturation corresponds to a power of about 1 mW absorbed within the ZnS powder. The scintillators have adequate time response up to 50-100 kHz.

I. INTRODUCTION

Scintillation detectors are used in the TFTR Tokamak to detect escaping charged fusion products.¹ Triton and proton fluxes of 10^8 - 10^9 $\text{cm}^{-2}\text{s}^{-1}$ are measured in D-D experiments and alpha fluxes of 10^{10} - 10^{11} $\text{cm}^{-2}\text{s}^{-1}$ are expected in D-T experiments. So far, only ZnS(Ag) has been used, but ZnS(Cu) is considered for future experiments.² The light output of these scintillators has been studied in some detail³ at fluxes of about 10^3 $\text{cm}^{-2}\text{s}^{-1}$. Further work at higher fluxes is required for a quantitative information from this diagnostic. Specific issues to be investigated are light output linearity, radiation damage, efficiency at high temperatures, and time response in the frequency range 0-1 MHz. In this paper, we report results obtained with a Curium radioactive source and with Van de Graaf ion beams that address some of the above issues.

II. EXPERIMENTAL APPARATUS

The scintillators are studied at the Los Alamos Ion Beam Facility in a vacuum chamber sketched in Fig.1. A ZnS powder of average thickness 9 ± 1 μ is deposited on a 2.5x2.5 cm quartz substrate. The scintillator is fixed in an Aluminum holder mounted on a stem that can be remotely moved up or down or rotated at any angle ϕ with respect to the ion beam direction. Measurements with the ^{244}Cm alpha source are made by placing the emitting surface 1 cm away from the scintillator rotated at $\phi = 180^\circ$. The Van de Graaf experiments are made with the ion beam entering from the left side on Fig. 1 through vertical and horizontal apertures. These apertures define rectangular cross sections sufficiently small that the beams are fully intercepted by the scintillator. For all experiments reported here, ϕ was set at 20° to simulate the TFTR experimental cases.¹ Before and after each

measurement, the scintillator is lowered to measure the beam current with a large area Faraday cup shown in Fig. 1.

The emitted light is collected by a train of three lenses designed to image the scintillator onto the photocathode of a photomultiplier tube (Hamamatsu R-762) with a magnification of 0.7. The PM tube is surrounded by a magnetic shield case and by a light-tight container. The output of the PM tube is connected to a preamplifier (Thorn EMI A1-101) . The amplified anode current is measured on a storage oscilloscope (Tektronix 2330) with a 50 Ω termination. The vacuum chamber has negligible stray light and is typically pumped down to 10^{-6} Torr. An observation port indicated in Fig. 1 is used to check the beam position on the scintillator with a video camera .

III. RADIOACTIVE SOURCE RESULTS

The light emitted by the scintillator is assumed to be proportional to the energy deposited into the phosphor by the charged particles.¹ This assumption is tested by inserting Aluminum foils of various thicknesses between the Curium source and a P-11 ZnS(Ag) scintillator. The relative light output measured as function of the foil thickness δ is indicated with solid circles in Fig. 2. A simple calculation of the energy deposited into the scintillator as function of δ is also shown with a solid line in Fig. 2. The calculation assumes that the alpha energy distribution is a Gaussian of 3.7 MeV central energy and of 1.4 MeV (FWHM) width. This distribution is an approximate fit to measurements made with a surface barrier diode. The model shows reasonable agreement with the data in Fig. 2. Presumably, an even better agreement could be obtained by including opacity³ and angular scattering effects. A maximum in light output is obtained for $\delta = 1.5 \mu$ rather than for $\delta = 0$ because the mean alpha range somewhat exceeds the average scintillator thickness viewed from the source. The results in Fig. 2 suggest that the emitted light is indeed approximately proportional to the energy deposited into the ZnS phosphor.

The linearity of the scintillator light output as function of the alpha particle flux is also studied by varying the distance between the Curium source and the scintillator. For each distance in the range 0.2 to 8 cm, the alpha flux is computed from the measured source activity of $\approx 2 \times 10^7 \text{ s}^{-1}$ and from the solid angle to the scintillator boundary. The oscilloscope voltage as function of alpha flux is shown with solid circles in Fig. 3. These data are obtained with a PM tube voltage of 0.5 kV, a preamplifier gain of 2×10^4 , and a blue filter (Corion P70-450-S) in front of the photocathode. The arbitrary straight line in Fig. 3 suggests that the emitted light is proportional to the alpha flux in the range 10^4 - $10^6 \text{ cm}^{-2}\text{s}^{-1}$.

IV. VAN DE GRAAF RESULTS

A. BEAM CURRENT DEPENDENCE

The P-11 ZnS(Ag) and the P-31 ZnS(Cu) scintillators are studied with 3.5 MeV alphas and 3 MeV protons beams in the range 10^{-11} to 10^{-7} A. These data are shown in Figs. 4 and 5. The oscilloscope voltages, proportional to the emitted light, are shown as functions of beam current. The corresponding particle fluxes are also indicated. The data in Figs. 4 and 5 are obtained with a PM tube voltage of 0.2 kV, a preamplifier gain of 2×10^4 , and apertures 0.4 by 0.4 cm that yield an area A of about 0.5 cm^2 on the scintillators oriented at $\phi = 20^\circ$. The data shown with hollow symbols correspond to chopped (10 ms on, 90 ms off) beams.

The scintillator light output first increases linearly with beam current and then saturates in Figs. 4 and 5. Similar saturations with ZnS(Ag) have been noted with 10-30 keV electrons beams⁴, with onsets at power densities of a few mW/cm^2 . The onset of the saturations in Figs. 4 and 5 correspond to absorbed power densities $\Delta E I_0 / Z e A$ of $1.4 \text{ mW}/\text{cm}^2$, where ΔE (3.5 MeV for alphas and 0.8 MeV for protons) is the energy deposited within the ZnS powder, Z is the atomic number, and I_0 (0.4 nA for

alphas and 0.9 nA for protons) is the onset current. However, other current scans with $A = 0.15$ and 2.3 cm^2 suggest that the saturations start at a constant 0.7 mW absorbed power. The cause of the above saturations remains unclear. Aside from possible instrumental problems, the potential main causes are: (1) radiation damage, (2) heating of the scintillator, (3) charge accumulation, and (4) saturation of the luminescent centers.

Radiation damage somewhat contributes to the saturations, as can be seen by comparing data with steady and chopped beams in Figs. 4 and 5. The scintillators are exposed for 60-100 s at each current, resulting in final fluences of $(2-3) \times 10^{13} \text{ cm}^{-2}$ for steady beams and of $(2-3) \times 10^{12} \text{ cm}^{-2}$ for chopped beams in Fig. 4. The scintillating efficiencies decrease permanently by about 20% after $3 \times 10^{12} \alpha/\text{cm}^2$ and by 60-70% after $3 \times 10^{13} \alpha/\text{cm}^2$, in rough agreement with previous results.² Scintillator heating does not appear to contribute much to the observed saturations. The temperature of the back of the scintillator was monitored with a thermocouple and did not increase by more than 50 °C at the highest current levels. In addition, energy estimates suggest that the ZnS temperature could not increase by more than 10-20 °C at the onset of the saturations. Charge accumulation at the surface and within the scintillator may contribute substantially to the observed saturations.⁴ The video recordings show a gradual transition from well-defined to diffuse impacted areas as the current is increased. Occasional sparks are observed at high currents. Various tests are under way to explore the influence of charge build-up. Saturation of the luminescent centers may also contribute to the observed saturations.

For a given flux within the linear current ranges, the emitted light is about 5 times larger for alphas in Fig. 4 than for protons in Fig. 5. However, this factor is mostly accounted for by the difference in ΔE . For given conditions, P-31 yields about half as much light as P-11, but most of this factor comes from the reduced PM tube efficiency (60%) in the green relative to the blue.

B. TIME RESPONSE

A slow chopper, already introduced in the context of Figs. 4 and 5, shows that both P-11 and P-31 have excellent time responses in the range 0-1 kHz. A fast chopper is used to extend these studies up to 1 MHz. Current pulses of 1 μ s duration and with rise and decay times of a few ns are produced at selected time intervals. An example with 12.8 μ s period is shown in Fig. 6(a) from a fast Faraday cup. The responses of the P-11 and P-31 scintillators to this current waveform are shown in Figs. 6(b) and 6(c), respectively. These traces are obtained with the lowest preamplifier gain which yields a 20 ns risetime. Both responses are qualitatively similar, with a relatively fast rise and a slower decay time. Both rise and decay include a fast initial component and a subsequent slower component. These are consistent with the fluorescence and phosphorescence processes.⁴ The slow decay times limit the resolution of high-frequency signals. One can crudely attribute a single exponential decay time to each scintillator by considering the ratios of maximum to minimum signals in Figs. 6(b) and 6(c). One obtains 9 μ s for P-11 and 18 μ s for P-31. These decay times were obtained at 0.75 nA peak current, and did not change appreciably at 75 pA and at 7.5 nA. The P-11 and P-31 scintillators can approximately detect oscillations of frequency less than 100 and 50 kHz, respectively. This is adequate for most but not all instability-induced oscillations (0-1 MHz) that may be present in TFTR and other Tokamak discharges.²

V. CONCLUSIONS

The studies with 3.5 MeV alphas and 3 MeV protons presented in this paper show that the light emitted by ZnS scintillators first increases linearly with beam current and then saturates. These saturations start at a power of about 1 mW into the ZnS powder. The escaping fusion products detected in present TFTR D-D experiments lie well within the linear response. However, some saturation of the emitted light is to be expected in future TFTR D-T experiments. Severe saturation and radiation damage

would occur in future larger Tokamaks. The losses of charged fusion products may be modulated at frequencies of up to 1 MHz by various instabilities. The ZnS scintillators should allow adequate resolution up to 50-100 kHz.

ACKNOWLEDGMENTS

The authors are indebted to Rita Gribble, Dick Scarberry, and to the staff of the Los Alamos Ion Beam Facility for excellent technical assistance.

This work was supported by the U.S. DOE.

REFERENCES

1. S.J. Zweben R.L. Boivin, M. Diesso, S. Hayes, H.W. Hendel, H. Park, and J.D. Strachan, Nucl. Fusion **30**, 1551 (1990).
2. S.J. Zweben, R. Boivin, S.L. Liew, D.K. Owens, J.D. Strachan, and M. Ulrickson, Rev. Sci. Instrum. **61**, 3505 (1990).
3. R.L. Boivin, Ph.D. Thesis, Princeton Plasma Physics Laboratory (1991).
4. V.L. Levsnin et al., in "Soviet Researches on Luminescence", Transactions of the Lebedev Physics Institute, Vol. 23, edited by Acad. D.V. Skobel'tsvn, Consultants Bureau, NY, 1964.

FIGURE CAPTIONS

Fig. 1 Sketch of the experimental apparatus.

Fig. 2 Relative light output as function of the Aluminum foil thickness placed in front of the alpha source.

Fig. 3 Oscilloscope voltage as function of the alpha particle flux from the Curium source.

Fig. 4 Oscilloscope voltage as function of beam current for 3.5 MeV alphas. The dotted lines outline departures from linearity. The solid and hollow symbols are for steady and chopped beams, respectively.

Fig. 5 Oscilloscope voltage as function of beam current for 3 MeV protons. The dotted curves outline departures from linearity. The solid and hollow symbols are for steady and chopped beams, respectively.

Fig. 6 Voltage traces showing (a) a chopped 3 MeV proton beam current, (b) the response of the P-11 scintillator, and (c) the response of the P-31 scintillator.

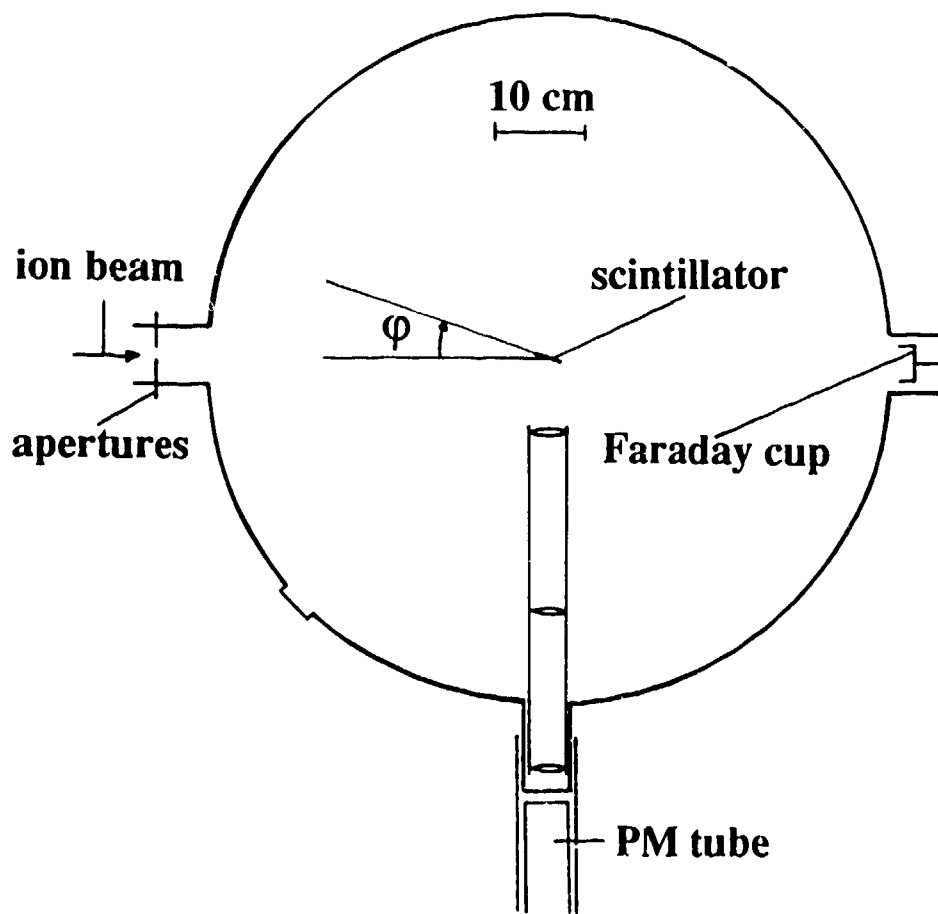
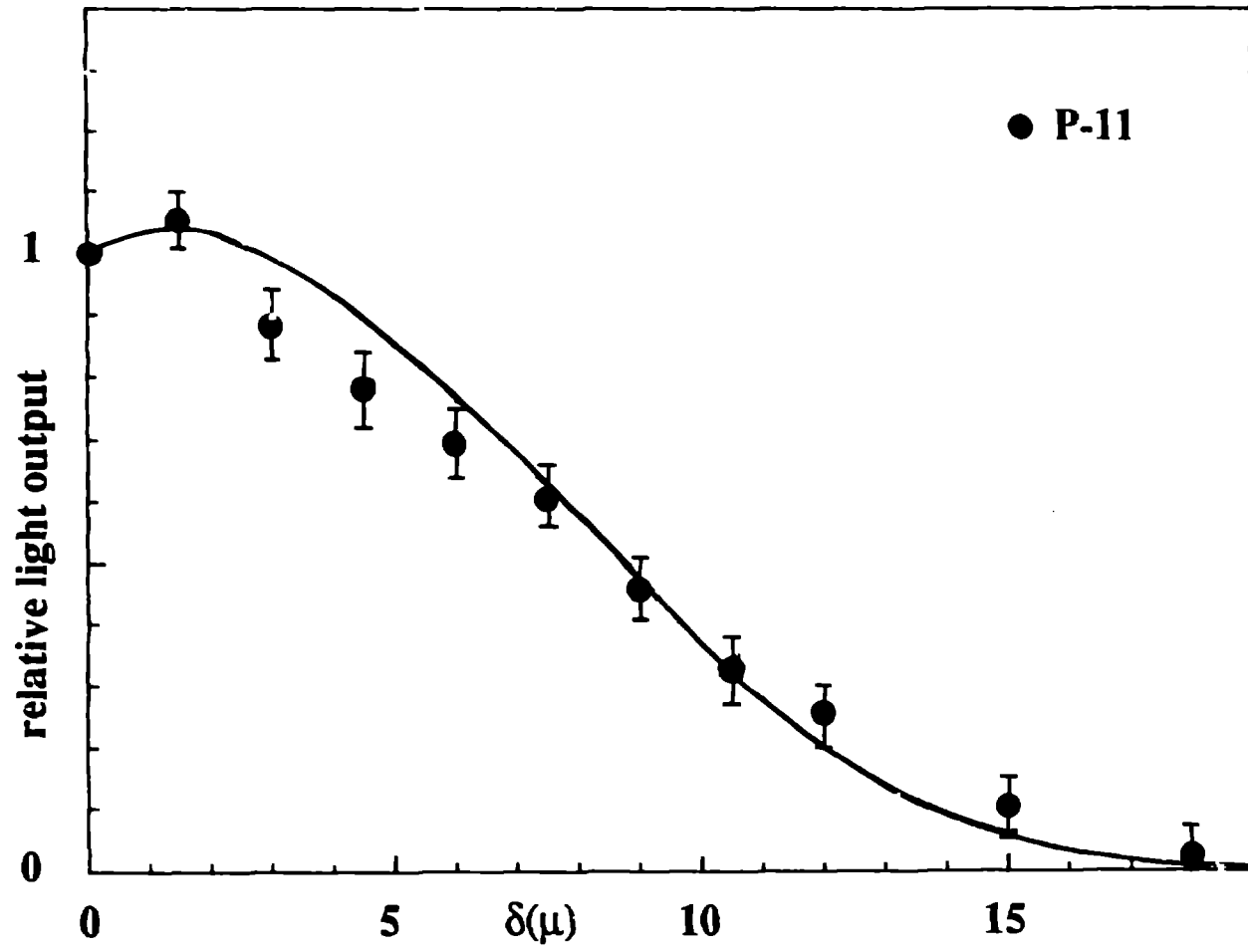


Fig. 1

Fig. 2



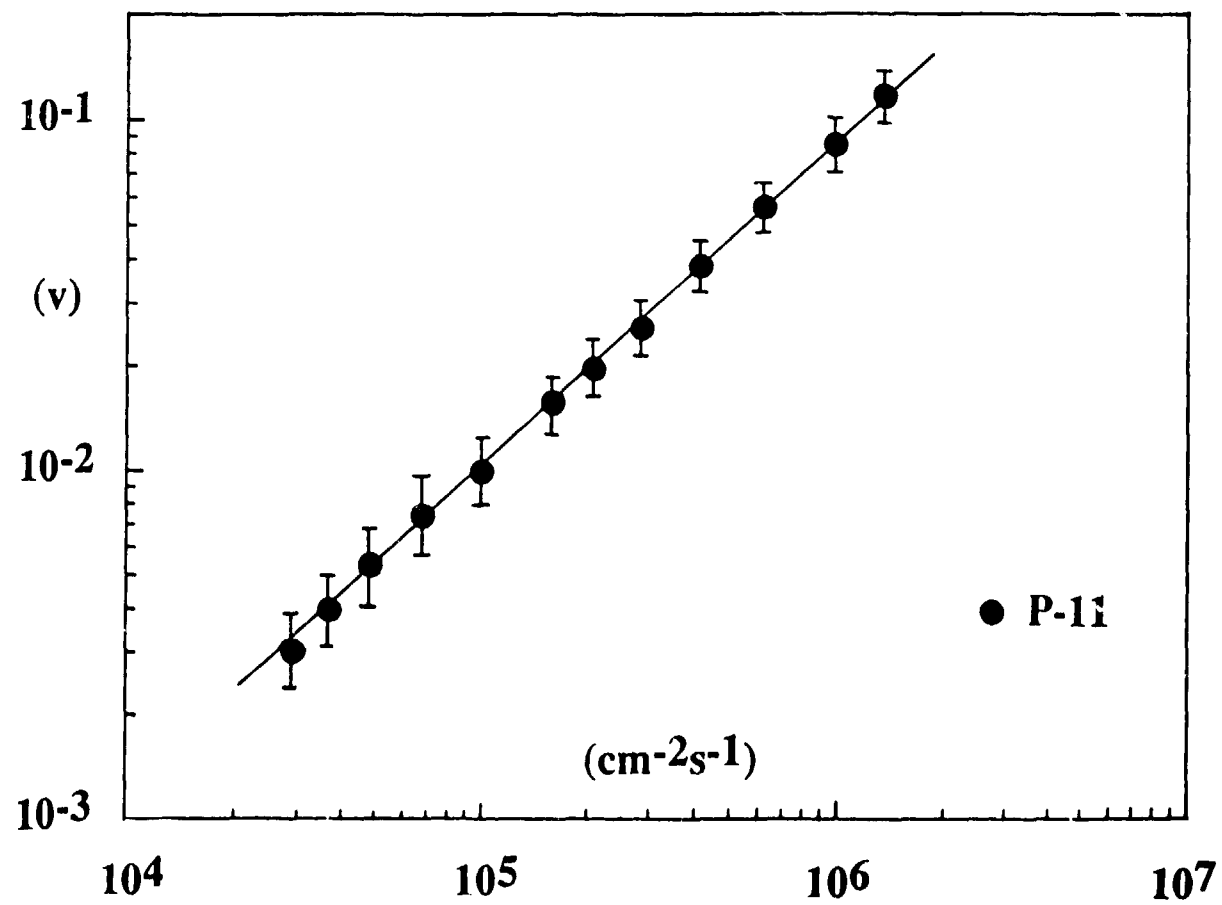


Fig. 3

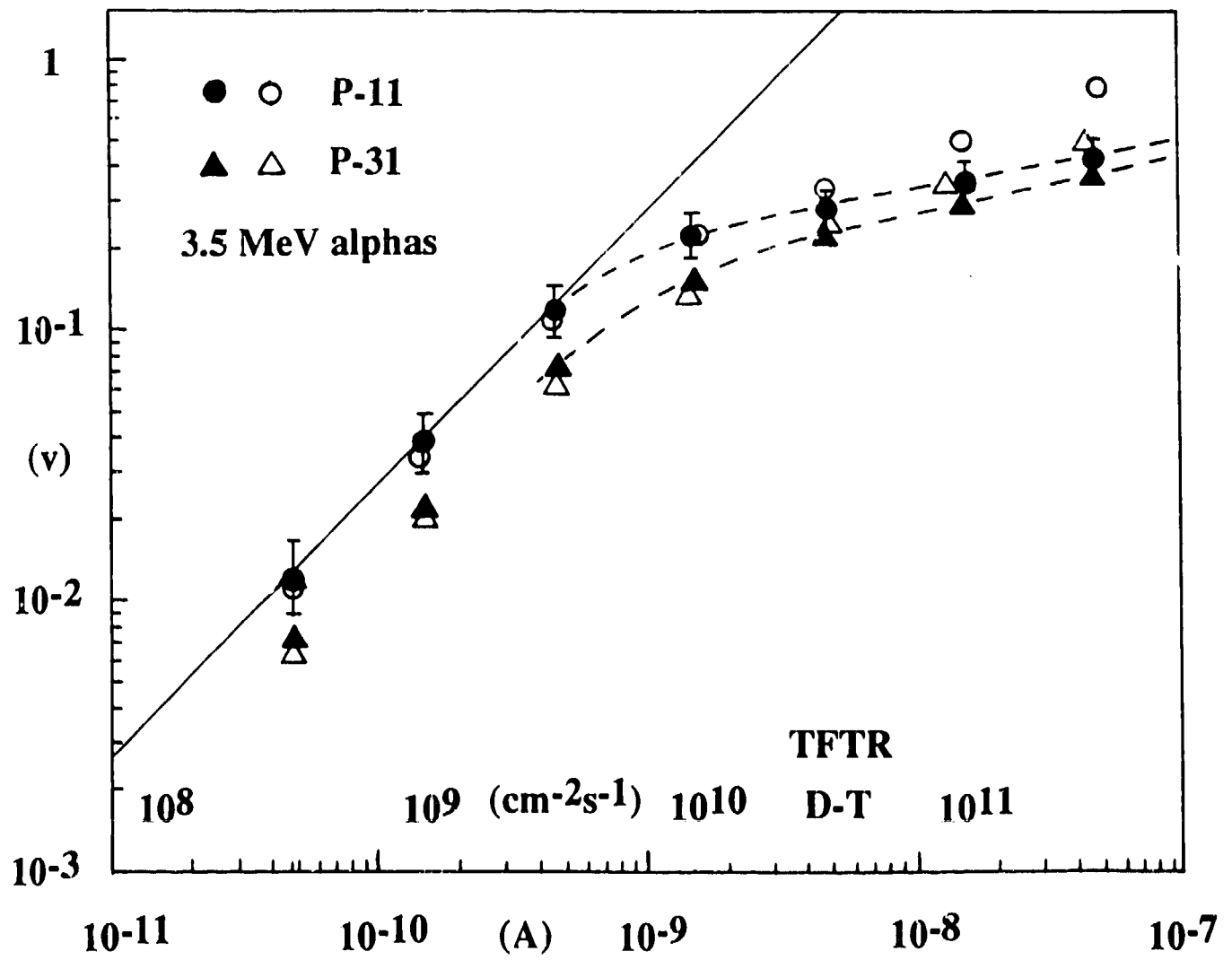


Fig. 4

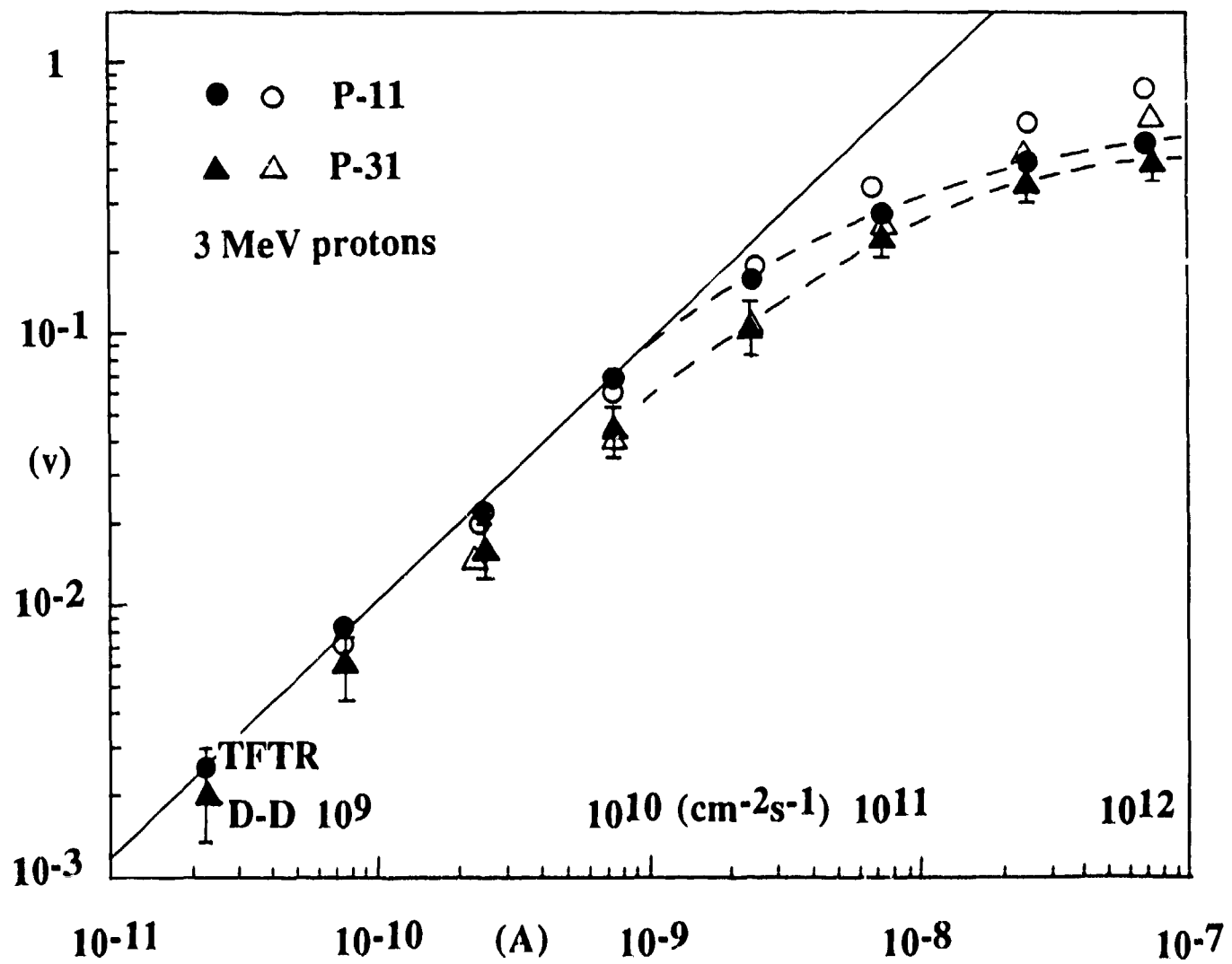


Fig. 5

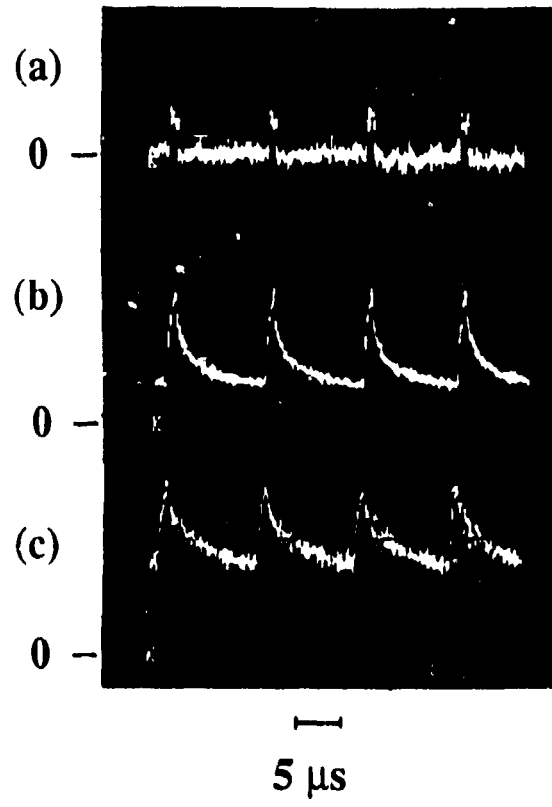


Fig. 6